

FIG. 1. Analytical startup curves.

plotted in Fig. 1. To compare these results with those obtained by the use of pump characteristic curves, Eqs. (7) and (8) were applied to a single suction Voith pump, and a double suction DeLaval pump. The characteristics of these pumps are represented by the polynomials given in Table 1 of reference 1.

The curves obtained from the analytical solution and from the characteristic curve solutions show similar flow startup patterns. For small values of the half-time ratio α the correspondence is very close. This is to be anticipated since low values of α indicate high inertia impellers which require a longer time to be brought up to steady-state operating speed. During this period, the fluid is brought up slowly to steady-state flow, with the result that there is no large change in the ratio of speed of pump to velocity of flow. The constant-characteristic-based analytical solution assumes that this ratio remains constant. Therefore, for small values of α the condition is closely satisfied.

Large values of α imply the presence of impellers with low inertia. During constant torque startup, such impellers would approach steady-state operating speed much more rapidly than the flow would approach steady-state flow. This produces a higher pressure across the pump than there would be if the flow increased proportionately with pump speed. The higher head across the pump would then accelerate the flow and accomplish the startup transient more rapidly than the analytical constant-characteristic solution would indicate. This was observed in comparing the analytical curves for high α with the true characteristic curves. From a practical point of view this discrepancy is not important, since with very light impellers the flow is established so rapidly that it is substantially a step jump. In view of this, the curves in Fig. 1 should give a fair estimate of the startup flow transient under constant impeller torque.

REFERENCE

1. D. BURGEEEN, Flow coastdown in a loop after pumping power cutoff. *Nuclear Sci. and Eng.* **4**, 306 (1959).

DAVID BURGEEEN

Nuclear Development Corporation of America
White Plains, New York

Received January 18, 1960

Spatial Distribution of Resonance Absorption in Fuel Elements

The spatial distribution of resonance absorption in fuel elements is a problem of high importance in reactor calculations. Usually most investigators (1, 2) have used Monte-Carlo methods which are very time-consuming and do not permit general conclusions. In this note an analytic approach to the problem is presented which leads to simple results and may well be generalized for similar applications.

The energy variation of cross section for strong resonance absorbers such as U^{238} may be described by a succession of Breit-Wigner resonances. Now, if it is possible to evaluate the spatial distribution of resonance absorption which may be attributed to some isolated resonance, one may expect the total absorption to be describable in terms of contributions from individual resonances.

Let us consider a cylindrical lump, immersed in moderator, which contains a strong resonance absorber uniformly

distributed in the interior of the lump. We shall require that the condition holds

$$\Sigma_0 R \gg 1 \quad (1)$$

where $2R$ is the diameter of the cylindrical fuel rod and Σ_0 the macroscopic absorption cross section at resonance energy. The source distribution of resonance neutrons will be assumed to be homogeneous and isotropic within the total moderator volume. This latter assumption may equivalently be expressed as follows: Resonance neutrons passing through the interface are distributed according to

$$q dE = \frac{S^*}{E} \cdot \frac{\cos \theta}{2\pi} dE \quad (2)$$

where θ is the angle between the normal to the surface and the direction of the neutron. It is further assumed that the epithermal flux spectrum satisfies the asymptotic $1/E$ dependence.

Basic to our procedure is the acceptance of first collision theory, that is, scattering in the absorber lump is completely neglected. Similarly Doppler-broadening of resonances is also ignored.

The resonance absorption at a distance r from the axis is given by

$$A(r) = \Sigma_0 \frac{\Gamma}{2} \int_{-\infty}^{\infty} \varphi(r, \xi) \frac{d\xi}{1 + \xi^2} \quad (3)$$

Here $\xi = [(E - E_0)/\Gamma/2]$ and

$$\varphi(r, \xi) = \frac{S^*}{E_0} \cdot \frac{R^2}{2\pi} \int_0^{2\pi} \int_{-\infty}^{\infty} \exp \left\{ -(\rho^2 + z^2)^{1/2} \frac{\Sigma_0}{1 + \xi^2} \right\} \cdot \frac{1 - \frac{r}{R} \cos \epsilon}{(\rho^2 + z^2)^{3/2}} d\epsilon dz \quad (4)$$

with

$$\rho^2 = R^2 \left(1 + \left(\frac{r}{R} \right)^2 - 2 \frac{r}{R} \cos \epsilon \right)$$

Notice the fact that integration over the resonance (variable ξ) may be performed before surface integration.

If the variable u from the expression

$$z = \rho \sinh u$$

is introduced, it can be shown that

$$\int_{-\infty}^{\infty} \exp \left\{ -\frac{\Sigma_0 \rho}{1 + \xi^2} \cosh u \right\} \frac{d\xi}{1 + \xi^2} = \pi \exp \left\{ -\frac{\Sigma_0 \rho}{2} \cosh u \right\} I_0 \left(\frac{\Sigma_0 \rho}{2} \cosh u \right) \quad (5)$$

From condition (1) for distances r satisfying the inequality

$$(R - r)\Sigma_0 \gg 1 \quad (6)$$

the asymptotic expression of the modified Bessel function I_0 may be used

$$I_0(x) \rightarrow \frac{e^x}{(2\pi x)^{1/2}} \left\{ 1 + \frac{1}{8x} + \dots \right\} \quad (7)$$

If only the main term is retained one arrives at

$$A(r) = \Sigma_0 \frac{\Gamma/2}{E_0} \cdot \frac{S^*}{\sqrt{\pi \Sigma_0 R}} \int_0^{2\pi} \frac{1 - \frac{r}{R} \cos \epsilon}{\left(1 + \left(\frac{r}{R} \right)^2 - 2 \frac{r}{R} \cos \epsilon \right)^{5/4}} d\epsilon \int_0^{\infty} \frac{du}{\cosh^{5/2} u} \quad (8)$$

the last integral contributing the factor 0.8740. The spatial distribution in the interior of the cylindrical fuel element, therefore, is given in the form

$$A(r) = \frac{A^*}{\sqrt{\Sigma_0 R}} f \left(\frac{r}{R} \right) \quad (9)$$

with

$$A^* = \Sigma_0 \frac{\Gamma/2}{E_0} \cdot S^* \cdot \frac{0.8740}{\sqrt{\pi}}$$

For strong resonance absorbers like U^{238} , Σ_0 is of the order of 10^3 . Therefore the asymptotic expression is valid in the whole volume apart from a thin surface layer.

The result [Eq. (9)] is surprising and important. It means that the radial distribution in cylindrical lumps for any resonance is given by a universal function $f(r/R)$, irrespective of the parameters of individual resonances. The radial function $f(r/R)$ is defined by

$$f(k) = \int_0^{2\pi} \frac{1 - k \cos \epsilon}{(1 + k^2 - 2k \cos \epsilon)^{5/4}} d\epsilon \quad (10)$$

Using the integral representation (3)

$$F(v, n + v; n + 1; z^2) = \frac{z^{-n} \Gamma(v) \Gamma(n + 1)}{2\pi \Gamma(n + v)} \int_0^{2\pi} \frac{\cos nt dt}{(1 + z^2 - 2z \cos t)^v} \quad (11)$$

$f(k)$ is given in terms of the hypergeometric series

$$f(k) = 2\pi [F(\frac{5}{4}, \frac{5}{4}; 1; k^2) - \frac{5}{4} k^2 F(\frac{5}{4}, \frac{5}{4}; 2; k^2)] \quad (12)$$

Figure 1 shows the behavior of the radial function $f(k)$. An obvious generalization leads to similar functions for other geometries:

Slab (thickness $2d$):

$$A(x) = \frac{A_1^*}{\sqrt{\Sigma_0 d}} f_1 \left(\frac{x}{d} \right) \\ f_1(k) = \frac{1}{\sqrt{1 - k}} + \frac{1}{\sqrt{1 + k}} \\ A_1^* = \Sigma_0 \frac{\Gamma/2}{E_0} \cdot \frac{2}{3} \sqrt{\pi} \quad (13)$$

Sphere:

$$A(r) = \frac{A_2^*}{\sqrt{\Sigma_0 R}} f_2 \left(\frac{r}{R} \right) \\ f_2(k) = \frac{2}{3k} \left\{ \frac{1 + 2k}{\sqrt{1 + k}} - \frac{1 - 2k}{\sqrt{1 - k}} \right\} \\ A_2^* = \Sigma_0 \frac{\Gamma/2}{E_0} \sqrt{\pi} \quad (14)$$

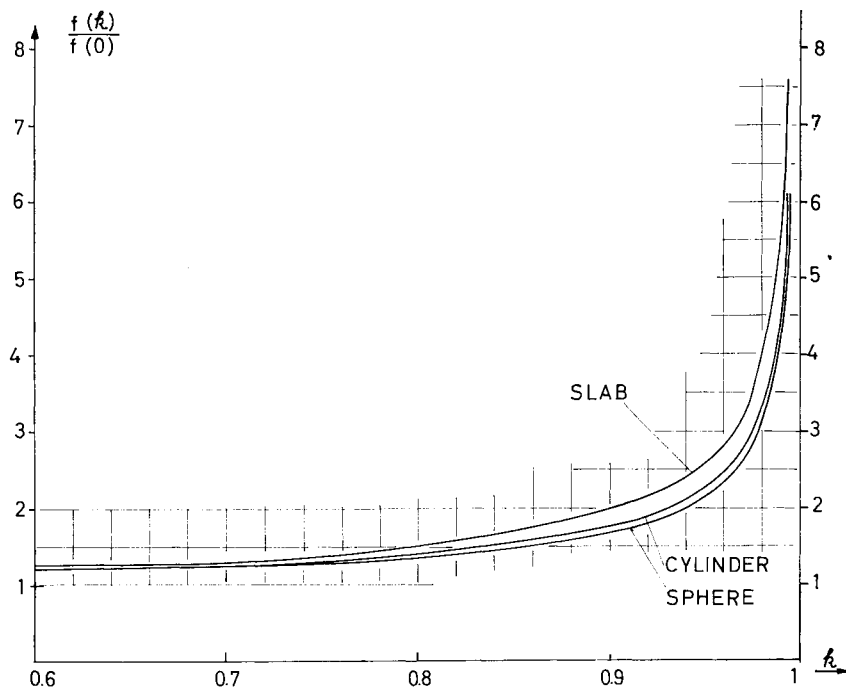


FIG. 1. Spatial distribution of resonance absorption in different geometries; slab, cylinder, sphere.

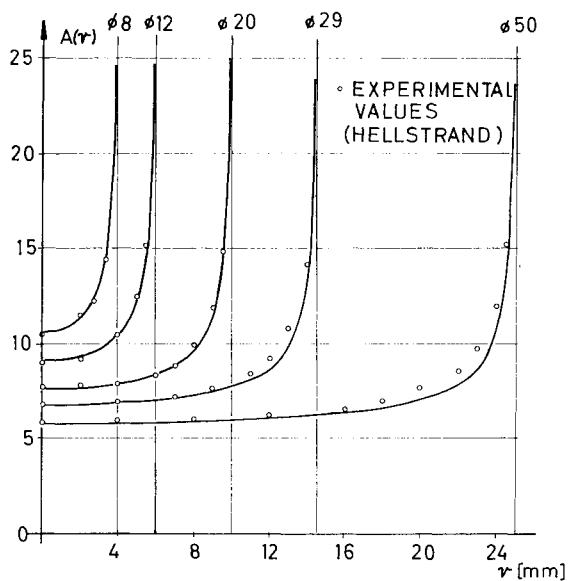


FIG. 2. Radial distribution of resonance absorption in cylindrical rods of different diameters. Comparison of calculated curves with measurement.

It should be noted that both the cylindrical and spherical distributions show the same asymptotic behavior $x^{-1/2}$ near the boundary which is characteristic of the slab case.

The results given may be compared with experimental data published by Hellstrand (4). Figure 2 shows the radial distribution of resonance absorption measured by the neptunium activity in irradiated rods of different diameters. A constant volume absorption corresponding to a volume contribution of 2.59 barn to the effective resonance integral

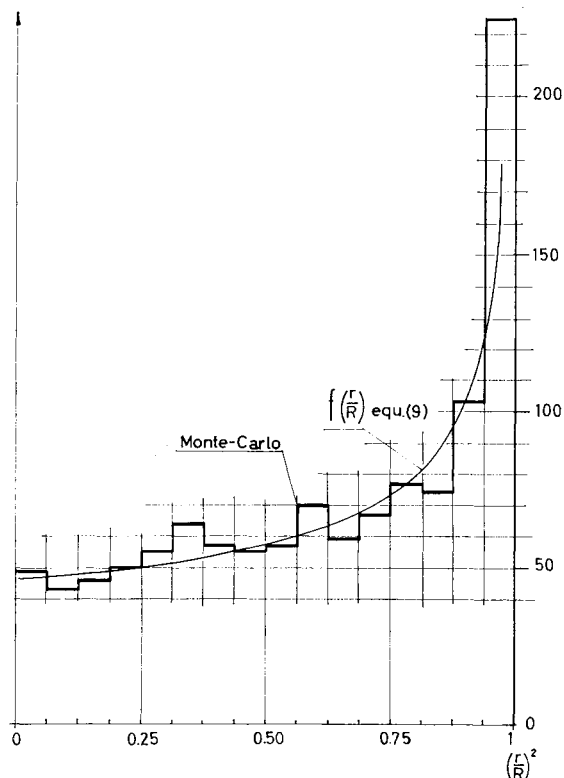


FIG. 3. Resonance absorption in a fuel rod ($R = 1.46$ cm). Comparison of First-Collision-Theory with Monte-Carlo results [Morton (2)].

has been adopted. The theoretical curves are calculated from Eq. (9), with the only requirement that the theoretical curve (rod diameter 8 mm) should agree with the experimental value for the point $r = 0$.

One further point of evidence comes from a comparison with Monte-Carlo calculations made by Morton (2), Fig. 3. In this case the analytic curve, without volume contribution, is shown. The Monte-Carlo results are derived under more realistic premises: Doppler-broadening of resonances, inclusion of resonance scattering, higher order collisions with energy degradation. The results, nevertheless, show the same trend as the "exact" distribution.

In the immediate vicinity of the surface the radial function no longer is independent from resonance parameters. For cylindrical rods one obtains

$$A(x) = \Sigma_0 \frac{\Gamma/2}{E_0} \cdot S^* \left\{ \pi F_2 \left(\frac{\Sigma_0 x}{2} \right) + \frac{1.8285}{\sqrt{\Sigma_0 R}} \right\} \quad (15)$$

in which $x = R - r$ is of the order $1/\Sigma_0$ and $F_2(\xi)$ is defined by

$$F_2(\xi) = \int_1^\infty e^{-\xi t} I_0(\xi t) \frac{dt}{t^2} \quad (16)$$

Männer and Springer (5) recently investigated the activation of plane resonance foils with similar methods and showed good correspondence with experimental results.

REFERENCES

1. R. D. RICHTMYER, BNL-433, p. 82 (1956).
2. K. W. MORTON, AERE-R 2929 (1959).
3. W. MAGNUS AND F. OBERHETTINGER, "Formeln und Sätze für die speziellen Funktionen der mathematischen Physik," p. 16. Springer, Berlin, 1948.
4. E. HELLSTRAND, BNL-433, p. 32 (1956); *J. Appl. Phys.* **28**, 1493 (1957).
5. W. MÄNNER AND T. SPRINGER, *Nukleonik* **1**, 337 (1959).

MANFRED WAGNER

c/o INTERATOM

Internationale Atomreaktorbau G.m.b.H.

Bensberg/near Cologne

Altes Schloss, Germany

Received February 25, 1960

A Note on the Perturbation Method in Neutron Transport Theory

In this note the perturbation formula of neutron transport theory (1-3) is derived by the method of ordinary perturbation theory used in quantum mechanics. Using the standard methods, formulas for higher order perturbations may be written down immediately.

As is well known the Boltzmann equation

$$\begin{aligned} \Omega \text{ grad } \psi(\mathbf{v}, \mathbf{r}) + \alpha(\mathbf{v}, \mathbf{r})\psi(\mathbf{v}, \mathbf{r}) &= q(\mathbf{v}, \mathbf{r}) \\ \gamma q(\mathbf{v}, \mathbf{r}) &= \int \beta(\mathbf{v}, \mathbf{v}'; \mathbf{r})\psi(\mathbf{v}', \mathbf{r}) d^3v' \end{aligned} \quad (1)$$

can be converted into an integral equation

$$\psi(\mathbf{v}, \mathbf{r}) = \int K^{(\alpha)}(\mathbf{v}; \mathbf{r}; \mathbf{r}') q(\mathbf{v}, \mathbf{r}') d^3r' \quad (2)$$

$$\gamma q(\mathbf{v}, \mathbf{r}) = \int \beta(\mathbf{v}, \mathbf{v}'; \mathbf{r})\psi(\mathbf{v}', \mathbf{r}) d^3v'$$

which in turn can be expressed in operator form

$$\begin{aligned} \psi &= K^{(\alpha)} q & \gamma q &= \beta \psi \\ \text{or } \gamma \psi &= K \beta \psi \end{aligned} \quad (3)$$

ψ being the directional flux, q the emission density, α the total cross section, $\beta(\mathbf{v}, \mathbf{v}'; \mathbf{r})$ the "transfer cross section" of neutrons of velocity \mathbf{v} into a velocity \mathbf{v}' lying in the element d^3v of velocity space. The eigenvalue γ which is the multiplication in one "scattering generation" is introduced instead of the reactivity. The kernels $K^{(\alpha)}$ and β possess the following symmetry properties:

$$\begin{aligned} K^{(\alpha)}(\mathbf{v}; \mathbf{r}; \mathbf{r}') &= K^{(\alpha)}(-\mathbf{v}; \mathbf{r}', \mathbf{r}) \\ \beta(\mathbf{v}, \mathbf{v}'; \mathbf{r}) &= \beta(-\mathbf{v}, -\mathbf{v}', \mathbf{r}) \end{aligned} \quad (4)$$

In order to prove the perturbation formula we further transform the Boltzmann equation into a new form. Defining

$$\beta^{(0)}(\mathbf{v}, \mathbf{v}'; \mathbf{r}) = (1/\gamma)\beta(\mathbf{v}, \mathbf{v}'; \mathbf{r}) - \alpha(\mathbf{v}, \mathbf{r}) \delta_{vv'} \quad (5)$$

the Boltzmann Eq. (1) becomes

$$\Omega \text{ grad } \psi(\mathbf{v}, \mathbf{r}) = q^{(0)}(\mathbf{v}, \mathbf{r})$$

$$q^{(0)}(\mathbf{v}, \mathbf{r}) = \int \beta^{(0)}(\mathbf{v}, \mathbf{v}'; \mathbf{r})\psi(\mathbf{v}', \mathbf{r}) d^3v' \quad (6)$$

which, in turn, can be written in operator form

$$\psi = K^{(0)} q^{(0)} \quad q^{(0)} = \beta^{(0)} \psi \quad (7)$$

or

$$\psi = K^{(0)} \beta^{(0)} \psi \quad \text{and} \quad q^{(0)} = \beta^{(0)} K^{(0)} q^{(0)}$$

We generalize these equations by introducing an eigenvalue ϵ ,

$$K^{(0)} \beta^{(0)} \psi_\epsilon = \epsilon \psi_\epsilon$$

and

$$\beta^{(0)} K^{(0)} q_\epsilon^{(0)} = \epsilon q_\epsilon^{(0)} \quad (8)$$

The physical solution for the flux ψ corresponds to the eigenvalue $\epsilon = 1$, all other solutions correspond to eigenvalues smaller than one. Two further equations with the same eigenvalues are formed with the transposed operators. Considering the symmetries (4), it is readily seen that the transposed of the equation for the emission density $q_\epsilon^{(0)}$ is equivalent to the Boltzmann equation (1) with β replaced by $(1/\epsilon)\tilde{\beta}$, α by $(1/\epsilon)\alpha$ and all the velocities reverted, i.e., the adjoint Boltzmann equation. The solutions $\psi_\epsilon^+(-\mathbf{v}, \mathbf{r})$ of the adjoint Boltzmann equation being eigenvectors of $(\tilde{\beta}^{(0)} K^{(0)})$ are orthogonal to the eigenvectors $q_\epsilon^{(0)}$ of (βK) belonging to different eigenvalues. This last fact can now be used to formulate perturbation theory in a straightforward manner.

$K^{(0)}$ is the matrix $K^{(\alpha)}$ for $\alpha = 0$ and is completely inde-